Astron. Astrophys. 138, 131–139 (1984)

ASTRONOMY AND ASTROPHYSICS

On the statistics of galactic H I clouds

K.R. Anantharamaiah[1], V. Radhakrishnan[1], and P.A. Shaver[2]

[1] Raman Research Institute, Bangalore 560 080, India
[2] European Southern Observatory, Karl-Schwarzschild-Strasse 2, D-8046 Garching bei München, Federal Republic of Germany

Received November 30, 1983; accepted March 8, 1984

Summary. The number density and random motions of interstellar H I clouds have been studied using an entirely novel method involving the comparison of the terminal velocities of H I absorption spectra in the direction of H II regions with their recombination line velocities. We confirm the conclusions of an earlier study attributing these velocity differences mainly to the random motions of the clouds. We also show that these motions are better described in terms of two populations with quite different velocity dispersions than by a single population with an exponential distribution of velocities. The present analysis yields estimates of the number densities and dispersions of $n_s = 7.7 \pm 1.8\,\mathrm{kpc}^{-1}$ $\sigma_s = 4.1 \pm 0.7\,\mathrm{km\,s}^{-1}$ for the "slow" clouds, and $n_f = 0.6 \pm 0.15\,\mathrm{kpc}^{-1}$, $\sigma_f = 15.2 \pm 3.2\,\mathrm{km\,s}^{-1}$ for the "fast" clouds. These values are compared with earlier estimates and the implications discussed. It is concluded that the values for the slow clouds are an improvement over earlier determinations, while those for the population of fast clouds are underestimates because of selection effects in the data used.

Key words: H I clouds – statistics – anomalous motions – interstellar matter

1. Introduction

The radial velocities of interstellar clouds do not conform strictly to the predictions of the Schmidt model of galactic rotation. This is because there are non-systematic or random motions in addition to the systematic circular motions around the centre of the galaxy. The magnitude of these random motions can in principle be estimated by comparing the measured radial velocities with the predicted radial velocities if the distances to the clouds somehow be determined independently. While this is almost impossible in practice for distant clouds in the galactic plane, a similar comparison can be made with H I absorption measurements against background continuum sources with independent radial velocity determinations. In such cases, one could compare the radial velocity of the background continuum source with the terminal velocity (corresponding to the greatest distance) of the H I absorption spectrum of the source. If there were no random motions, one would expect only the velocity difference corresponding to the distance between the background source and the H I cloud nearest to, and in front of it; the magnitude of this difference would depend on the galactic longitude.

Send offprint requests to: K.R. Anantharamaiah

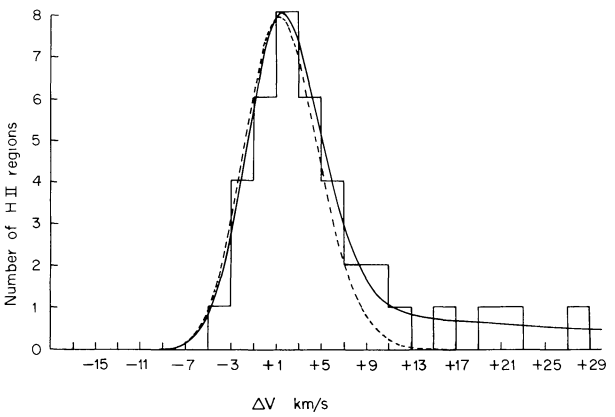

Fig. 1. (Taken from Shaver et al., 1982.) Histogram of the difference between the H 109α velocity and that of the extreme H I absorption feature (corresponding to the greatest distance) for 38 galactic H II regions. The dashed line is the fit obtained by Shaver et al. (1982) considering the dispersion of normal clouds only; the solid line includes the effect of a small fraction of clouds with much larger random motions

Shaver et al. (1982, hereinafter referred to as Paper I) have made such a comparison. The recombination line velocity of each of 38 H II regions of known distance was compared with the terminal velocity of its H I absorption spectrum (Table 1). Figure 1 shows a histogram of the velocity differences from Paper I. Shaver et al. (Paper I) found that in most (80%) of the cases, the velocity of the H I absorption feature corresponds paradoxically to a *greater* distance than that of the H II region. They have argued that this cannot be explained as due to random motions of H II regions, or streaming of ionized gas of the H II region away from the parent molecular cloud. The authors have sought an explanation for the distribution of the observed ΔV (the difference between the recombination line velocity and extreme H I velocity) in terms of the random motions of the absorbing H I clouds themselves. They showed that the observed anomaly is simply a consequence of such random motions, and that in these cases the values of ΔV must provide *lower limits* to such motions. On account of these motions, some clouds will appear to be beyond the H II region as illustrated in Fig. 2.

From many attempts to fit the histogram (Fig. 1) in terms of the random motions of H I clouds, it was concluded (Paper I) that the histogram can be fitted in its entirety only on the assumption that

Table 1. Parameters for the 38 H II regions[a]

Source		ΔV[b]		Distance[d]	(dv/dr)[e]
G	Optical	km s^{-1}	τ_{max}[c]	kpc	km s^{-1} kpc^{-1}
206.5−16.4	NGC 2024	+ 3.7	5.3	0.5	10.8
209.0−19.4	Orion	+ 8.3	1.05	0.5	11.4
243.1+0.4	RCW 16	+ 1.4	>0.7	4.2	12.5
265.1+1.5	RCW 36	+ 2.0	3.5	0.6	6.1
268.0−1.1	RCW 38	+ 5.3	4.3	0.6	6.6
274.0−1.1	RCW 42	− 3	~1.2	6.1	11.8
282.0−1.2		− 2.4	~1.0	6.6	11.3
284.3−0.3	RCW 49	+ 4.7	~3.0	6.0	9.5
298.2−0.3		− 2.4	~2.5	11.7	13.4
298.9−0.4		+ 0.8	~1.5	11.5	13.6
322.2+0.6	RCW 92	+ 4.2	~2.3	3.7	−13.5
326.6+0.6	Nebulosity	+ 2.5	~1.0	3.2	−14.6
327.3−0.6	RCW 97	+ 0.7	2.9	3.5	−14.6
330.9−0.4		+ 6.9	>0.9	4.2	−15.0
332.2−0.4		+ 1	~1.6	4.1	−15.0
333.1−0.4		− 0.9	2.2	4.1	−15.0
333.6−0.2	Nebulosity	+21.7	~1.2	3.7	−15.5
336.5−1.5	RCW 108	+ 1.1	~2.3	2.1	−12.5
337.9−0.5		+19.6	~0.3	3.5	−14.6
338.9+0.6		− 1	>1.2	5.2	−15.9
340.8−1.0	RCW 110	+ 3.2	~1.6	2.5	−11.5
345.4−0.9	RCW 117	+10.5	1.5	5.0	−11.0
345.4+1.4	Nebulosity	+ 9.4	~1.2	1.9	− 8.6
348.7−1.0	RCW 122	+ 27.2	0.2	2.0	−12.5
351.4+0.7	NGC 6334	+ 1.8	1.5	0.7	− 4.7
351.7−1.2		+16.5	3.5	2.6	− 9.6
353.1+0.7	NGC 6357	+ 0.9	~1.6	1.0	− 3.8
353.2+0.9	NGC 6357	+ 7.2	~1.0	1.0	− 3.8
6.0−1.2	M8	+12.4	0.44	1.0	3.5
12.8−0.2		0.0	2.9	4.6	11.2
15.0−0.7	M17	+ 4.6	~1.4	2.3	9.2
16.9+0.7	M16	− 5.0	1.3	2.7	9.9
25.4−0.2		+ 6.0	0.2	4.7	15.6
28.8+3.5	RCW 174	+ 6.5	2.5	0.1	12.6
30.8−0.0		+ 4.9	1.3′	7.0	6.2
34.3+0.1		+ 2.1	>1.2	3.8	14.3
35.2−1.8		− 2.2	3.5	3.4	14.5
111.5+0.8	S 158	+ 1.4	−	4.9	−12.3

[a] See Shaver et al. (1982) for references
[b] ΔV is positive when the H I velocity corresponds to a greater distance than that of the H 109α line
[c] τ_{max} is the optical depth of the extreme H I absorption feature
[d] Distances are based on recombination line velocity
[e] Computed near the H I region

there are two populations of H I clouds; the standard clouds easily seen in absorption and characterised by a gaussian velocity distribution with $\sigma \approx 5$ km s^{-1} ("slow"), and a smaller population with a much larger σ ("fast"). They also noted that while the dispersion of the slow clouds cannot be very different from the assumed value ($\sigma \approx 5$ km s^{-1}) there was considerable room (15–40 km s^{-1}) for varying the velocity dispersion and the number density of the fast population; when one was increased, the other had to be decreased to get a good fit to the histogram of Fig. 1.

In the simple analysis in Paper I, average values for the velocity gradients and number densities were implicitly assumed. In this paper we reanalyse the same data assuming only the general conclusion of Paper I, namely that there are two populations of H I clouds. In the next section we investigate the effect of random motions and number densities of H I clouds on the expected velocity differences by taking into account the velocity gradient and distance of each individual H II region. In Sect. III, we estimate the number densities and dispersion of random motions of the two

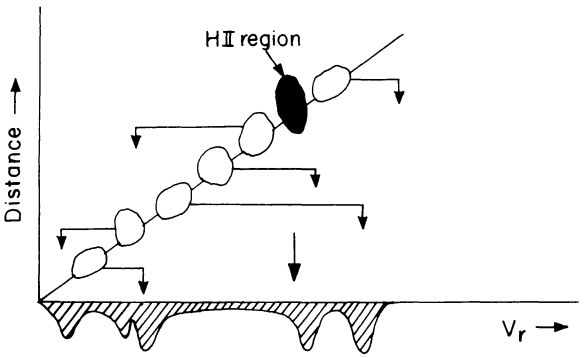

Fig. 2. Shematic representation of radial velocity of H I clouds (unfilled blobs) lying along the line of sight to an H II region. The hatched curve represents the H I absorption spectrum in that direction. Note that the true order in distance of the clouds is replaced by their order in velocity in the absorption spectrum due to their random motions (arrows)

populations of H I clouds from a least squares fit to the observed velocity differences ΔV. We also try a fit with a single exponential distribution of random velocities for the H I clouds, and show that even on the basis of this limited sample the two population hypothesis is to be preferred. Finally the implications of these results are discussed in Sect. IV.

II. Effect of velocity gradients, distances and random motions on H I terminal velocities

The influence of random motions on the velocity differences ΔV depends on the position of the H II region in the galactic disk as explained below. Consider for example an H II region in a direction close to that of the galactic centre for wich the radial velocity gradient $|dv/dr|$ will be very small. In such a situation, and in the absence of random motions, most of the clouds along the line of sight to the H II region will have nearly the same velocity as the H II region itself. Given random motions, then in principle nearly half of these clouds can have velocities corresponding to a greater distance than the H II region. If the distance to the H II region were increased, then the number of clouds which could masquerade as being more distant than the H II region will increase. On the other hand, if the velocity gradient is very large, only a few clouds will have systematic velocities close to that of the H II region; but if the random velocities are large enough, then some of these clouds could have velocities corresponding to a greater distance than the H II region. In such a situation, increasing the distance to the H II region will have a negligible effect on the number of clouds which could appear as being more distant. In other words. a small $|dv/dr|$ coupled with a large distance is what is required for a clear manifestation of the random motions in this fashion.

We will now illustrate this effect with a few real cases taken from the sample of 38 H II regions. Following Paper I, consider N H I clouds along the line of sight to an H II region. Let the velocity ΔV of the i^{th} H I cloud be governed by a Gaussian distribution with mean ΔV_i and standard deviation σ. ΔV_i is the systematic velocity difference between the H II region and the cloud. The probability distribution of $\Delta V_{\max}$ corresponding to the terminal velocity of the spectrum is then given by

$$P(\Delta V_{\max}) = \sum_{i=1}^{N}\left[p_i(\Delta V_{\max}-\Delta V_i)\prod_{j\neq i}^{N}\int_{-\infty}^{\Delta V_{\max}} p_j(\Delta V'-\Delta V_j)d\Delta V'\right], \quad (1)$$

where

$$p_i(\Delta V-\Delta V_i)=\frac{1}{\sigma\sqrt{2\pi}}\exp\left[-(\Delta V-\Delta V_i)^2/2\sigma^2\right].$$

Equation (1) is derived by assuming that any one of the clouds has a velocity $\Delta V_{\max}$ and the remainder have smaller velocities. Suppose now there are N_s slow clouds characterised by a dispersion σ_s, and N_f fast clouds with a dispersion of σ_f. The over-all probability distribution of $\Delta V_{\max}$ which we shall call ΔV is then given by

$$P(\Delta V)=\sum_{i=1}^{N_s}\left[p_{si}\prod_{j=i}^{N_s}\left\{\int_{-\infty}^{\Delta V}p_{sj}d\Delta V'\right\}\prod_{k=1}^{N_f}\int_{-\infty}^{\Delta V}p_{fk}d\Delta V'\right] + \sum_{i=1}^{N_f}\left[p_{fi}\prod_{j\neq i}^{N_f}\left\{\int_{-\infty}^{\Delta V}p_{fi}d\Delta V'\right\}\prod_{k=1}^{N_s}\int_{-\infty}^{\Delta V}p_{sk}d\Delta V'\right], \quad (2)$$

where

$$p_{si}=p_{si}(\Delta V-\Delta V_i)=\frac{1}{\sigma_s\sqrt{2\pi}}\exp\left[-(\Delta V-\Delta V_i)^2/2\sigma_s^2\right],$$

and

$$p_{fi}=p_{fi}(\Delta V-\Delta V_i)=\frac{1}{\sigma_f\sqrt{2\pi}}\exp\left[-(\Delta V-\Delta V_i)^2/2\sigma_f^2\right].$$

The N_s slow clouds and N_f fast clouds are assumed to be distributed uniformly but at random along the line of sight to the H II region. Then depending on its position, the systematic velocity difference ΔV_i for each cloud is given by the Schmidt model of galactic rotation. We derive in the Appendix a probability distribution Eq. (A2) for ΔV corresponding to Eq. (2) above, but taking full account of the distance and velocity gradient for each source. We show there that this is given by the convolution of a "window" function for each source with the probability distribution of peculiar velocities. Figures 3 and 4 show the probability distribution functions $P(\Delta V)$ computed for 6 of the H II regions taken from Table 1, using the Eq. (A2).

The figures marked a1, a2, a3 show $P(\Delta V)$ computed using $N_s=7.7d$ (where d is the distance to the source in kpc), $\sigma_s=4.1\,\mathrm{km\,s^{-1}}$ and $N_f=0$ (only slow clouds); the figures marked b1, b2, b3 show $P(\Delta V)$ computed using the same values of N_s and σ_s but with $N_f=0.6d$ and $\sigma_f=15.2\,\mathrm{km\,s^{-1}}$ (both slow and fast clouds). The choice of these numbers is explained in Sect. III. The figures marked c1, c2, c3 show the window functions $(1/|dv/dr|)$ as a function of velocity, and the arrows indicate the observed ΔV for the respective sources. G248.3–0.3 in Fig. 4 is an example of an H II region outside the solar circle for which the window function has a step at the solar circle velocity (see Appendix).

It is clearly seen in these figures that we cannot account for the high positive ΔV cases without introducing the second population of fast clouds with a high σ. It is also seen that dv/dr and the distances to the individual sources have in fact the expected effects on the probability distribution $P(\Delta V)$. The distributions and in particular their tails shift to more positive ΔV values as the area under the window function increases. For example, G348.7–1.0, G351.7–1.2 and G284.3–0.3, all of which have smalll values of $|dv/dr|$ and are at relatively large distance, have a long tail extending out to $\Delta V=30\,\mathrm{km\,s^{-1}}$, whereas G353.2+0.9 although it has a small $|dv/dr|$, has a very low probability for high positive ΔV due to its small distance. On the other hand, G333.6–0.2 has a large $|dv/dr|$ but still has a tail in the distribution due to its large distance, and in fact the observed ΔV for this source is $21.7\,\mathrm{km\,s^{-1}}$.

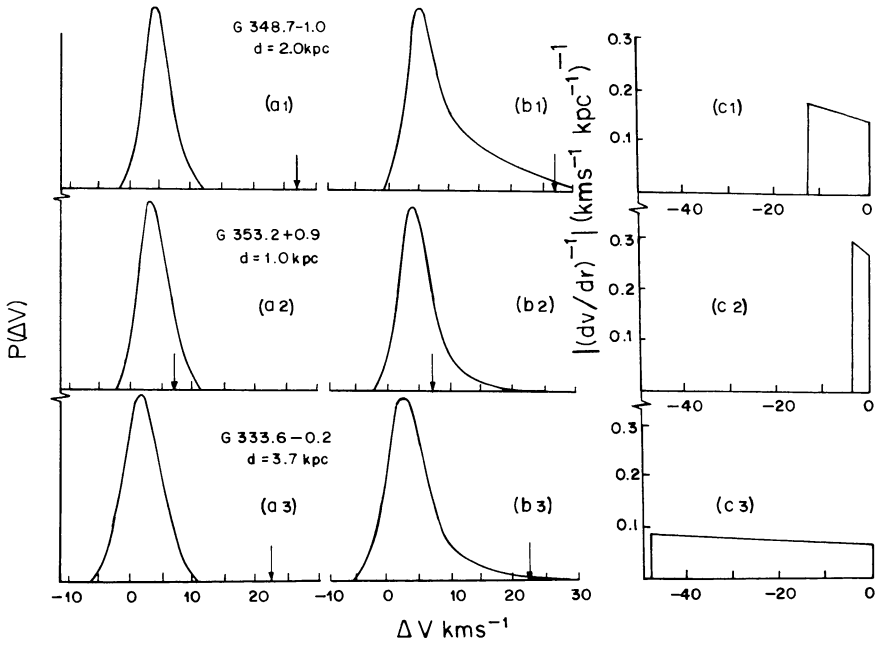

Fig. 3. The overall probability distributions of ΔV for different H II regions. (a1), (a2), (a3) are the distributions computed assuming that only slow clouds are present along the line of sight; (b1), (b2), (b3) show the effect on the distribution of including fast clouds. (c1), (c2), (c3) are the window functions for the respective sources and represent the probability distribution of systematic velocity for each cloud along the line of sight, according to the Schmidt model (see Appendix). The arrrows indicate the observed ΔV for the respective sources

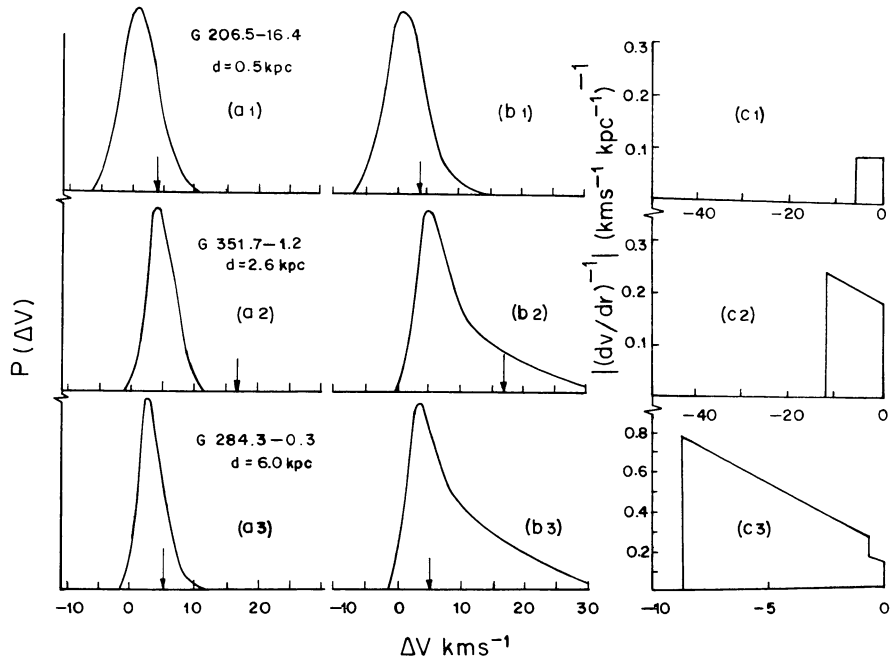

Fig. 4. Same as Fig. 3. Note that for G284.3–0.3 which is outside the solar circle, the value of $(dv/dr)^{-1}$ is doubled for the region between the tangential point and the solar circle because of velocity folding (see Appendix)

For G206.5–16.4, the addition of fast clouds has a negligible effect on the $P(\Delta V)$ distribution due to its small distance and large $|dv/dr|$.

It should be pointed out here that $P(\Delta V)$ is only a probability distribution and therefore the presence of a long tail extending to large positive ΔV's does not require that for these sources the observed ΔV should necessarily be large. The presence of a long tail shows that there is a finite probability of observing a large positive ΔV, and for those sources for which the tail is absent the probability of observing a large positive ΔV is extremely small. We have examined these probability distributions for all the 38 H II regions in Table 1 and find that for all those cases in which high positive ΔV's are observed, the distributions indeed have long tails as for G348.7–1.0 and G333.6–0.2 in Fig. 3. For six of the sources for which the observed ΔV is negative, the distribution extends to negative ΔV's. It may be noted that for several sources the expected distribution is practically restricted to positive ΔV's only.

It is clear that these tests confirm the conclusions drawn in paper I where the sample was treated as homogeneous. It appears established that the random motions of H I clouds and their number densities manifest themselves in the observed differences between recombination line velocities and the velocities of the

Table 2. Best fit values of H I cloud parameters

Velocity distribution	Cloud population	Dispersion or scale length km s^{-1}	Number density kpc^{-1}	Ψ^{2a}
2 Gaussian	Slow	4.1 ± 0.7	7.7 ± 1.8	45.5
	Fast	15.2 ± 3.2	0.6 ± 0.15	
Exponential	Single	4.4 ± 0.6	6.3 ± 1.4	72.2

[a] Indicates goodness of fit (see Appendix)

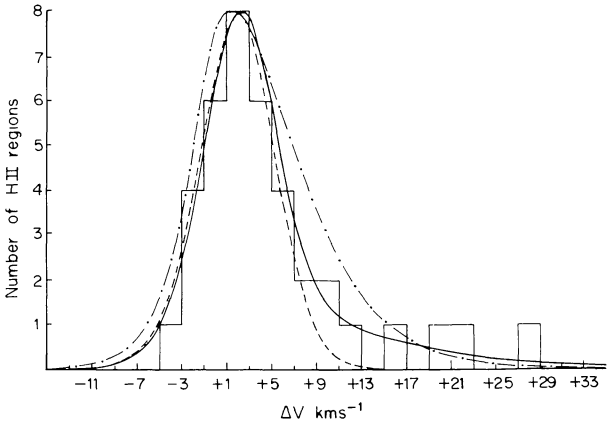

Fig. 5. The composite probability distribution for ΔV obtained by adding the individual probability distributions for the 38 H II regions in the histogram, computed using the best fit values of the cloud parameters (Table 2). The full curve is the distribution computed using both slow and fast clouds. In the dashed curve the effect of fast clouds has been removed; the parameters for the slow clouds are as in Table 2. The dashed and dotted curve is the distribution computed using an exponential distribution of random velocities. Note that the curves are drawn with their peak values normalized to the peak of the histogram

terminal H I absorption features. We can now ask how much more information we can get about these properties from the observed velocity differences in Table 1.

III. The number density and velocity dispersion of H I clouds

It was shown in Paper I and further confirmed from the tests described in Sect. II above that we need two populations of H I clouds with different random motions and number densities to account for the histogram of Fig. 1. If we assume that these two populations of H I clouds are randomly distributed throughout the Galaxy, we can then estimate the number densities (n_s and n_f) and velocity dispersions (σ_s and σ_f) from the observed ΔV's alone, to the accuracy permitted by the limited number in the sample.

Consider n_s slow clouds per kpc along the line of sight to an H II region with random motions characterised by a Gaussian dispersion σ_s, and n_f fast clouds per kpc with a dispersion σ_f. Then the probability of observing a velocity difference ΔV is given by Eq. (A2) in which $N_s = dn_s$ and $N_f = dn_f$ where d is the distance to the source in kpc. If ΔV_1, $\Delta V_2 \ldots \Delta V_{38}$ are the observed velocity differences for the 38 H II regions, then the individual probabilities of observing these differences are $P_1(\Delta V_1)$, $P_2(\Delta V_2) \ldots P_{38}(\Delta V_{38})$. The joint probability of observing these velocity differences is

$$P = \prod_{i=1}^{38} P_i(\Delta V_i). \tag{3}$$

We have maximised the quantity P by varying the four parameters n_s, σ_s, n_f and σ_f in an iterative procedure and obtained the best fit values. These values along with their errors and a measure of the goodness of fit are given in Table 2. (The estimation of errors and goodness of fit are discussed in Sect. II of the Appendix.) These were the values of the four parameters that were used in the tests described in Sect. II. Figure 5 shows the resulting predicted probability distribution (full line) for the histogram computed using these parameters; the dashed line is the probability distribution computed using only one population of (slow) clouds ($n_f = 0$). It can be seen that as noted in Paper I, the positive ΔV side of the histogram, including its long tail, requires the presence of the second population of fast clouds to give a good fit.

It is interesting that the inability of a single gaussian to fit the peculiar motions of interstellar clouds was noted even in the earliest study such as that of Blaauw (1952) who analysed the measurements of Adams (1949) to determine the distribution of radial motions. He concluded that the high radial velocities observed for many clouds could be better accounted for by an exponential distribution of velocities for interstellar clouds. Both for the sake of completeness and for its appeal of simplicity, we have also considered here the possibility of a single population of clouds with an exponential distribution of velocities accounting for the observed high velocity differences shown in Table 1.

Consider again n clouds per kpc distributed randomly along the line of sight to an H II region. Let the random velocity of each cloud be described by an exponential probability function of the form

$$P_{\text{ran}}(\Delta V - \Delta V_i) = A \exp(-|\Delta V - \Delta V_i|/\eta) \tag{4}$$

where η is the scale length of the distribution. As before, ΔV represents the difference between the velocity of the H II region and the cloud. The velocity distribution functions can be obtained in a similar fashion using Eq. (A1). Using these the probabilities $P_1(\Delta V_1)$, $P_2(\Delta V_2) \ldots P_{38}(\Delta V_{38})$ can be obtained from Eq. (A2) by replacing N_s by nd (d is the distance to H II region in kpc), and setting $N_f = 0$.

We have again maximized the joint probability P [Eq. (3)] in an iterative procedure by varying the parameters n and η. The best fit values of these parameters along with their errors and goodness of fit are given in Table 2. We have also shown in Fig. 5 the total probability distribution for the histogram computed on this basis (dots and dashes).

It can be seen both from Fig. 5 and from the goodness of fit values that the exponential distribution of radial velocities of a single population of H I clouds does not account for the observed velocity differences as well as the two-population hypothesis described earlier. It should be noted however, that the curves in Fig. 5 are a much poorer indication of the agreement between observation and prediction than the goodness of fit values. The latter represent a more stringent test involving the agreement in each individual case, as opposed to the general agreement with the total distribution of ΔV values in Fig. 5. Since it would be unwarranted at this stage to introduce more complicated distributions, we conclude from our analysis that the observed velocity differences in Table 1 can be best accounted for by two populations of H I clouds characterised by the number densities and velocity dispersions listed in Table 2.

IV. Discussion

We discuss below separately the characteristics of slow and fast clouds obtained from the above analysis.

Slow clouds

The slow clouds fall into the category of standard clouds very easily seen in 21 cm absorption studies and discussed by Radhakrishnan and Goss (1972). Our value for the slow cloud number density of $7.7 \pm 1.8\,\mathrm{kpc}^{-1}$ is about 3 times that (2.5–$3\,\mathrm{kpc}^{-1}$) estimated from a statistical analysis of the Parkes 21 cm absorption survey (see Radhakrishnan and Goss, 1972 and references therein). It may seem intriguing at the outset that different number densities are obtained from two analyses of essentially the same data, since most of the H I absorption measurements of Table 1 were also taken from the Parkes survey (see Paper I). However, the statistical analysis of Radhakrishnan and Goss (1972) suffered severely from blending of absorption features in velocity space as was noted by them.

If the number density of slow clouds is as high as indicated by the present analysis, then we may expect considerable blending of features in any H I absorption measurements irrespective of the velocity resolution used. Further, as discussed and emphasised by Radhakrishnan and Srinivasan (1980, hereafter R&S), the estimates from optical observations have always been even higher, typically 10–$20\,\mathrm{kpc}^{-1}$. It is to be expected therefore that a Gaussian analysis of the H I profiles would yield a smaller number density than the true value. In the present analysis of the differences in the velocity of the recombination line and that of the extreme H I *absorption* feature, we are working in a special region of velocity space where such blending is unlikely or very small. We therefore believe that our number density for the slow clouds is more accurate than earlier determinations.

While the velocity dispersion for the slow clouds obtained by us is in reasonable agreement with earlier determinations, it happens to be the smallest yet. The value of σ_s is $4.1 \pm 0.7\,\mathrm{km\,s}^{-1}$ as given in Table 2, whereas earlier estimates for it have been somewhat higher; for example, Crovisier (1978) obtained $5.7 \pm 0.9\,\mathrm{km\,s}^{-1}$ (see that paper also for a discussion of previous determinations). Crovisier points out the difficulty of discriminating between a gaussian and an exponential distribution from his sample, and notes the presence of higher-velocity features the inclusion of which suggests the tail of an exponential. While choosing a gaussian distribution obtained by excluding these features, Crovisier in fact suggested that these higher-velocity clouds may belong to another population.

If there are really two populations, then it is only to be expected that the dispersion obtained by treating the data as belonging to a single population will tend to be higher through contamination of the sample. Radhakrishnan and Sarma (1980, hereafter RS) quote a dispersion of $4.8 \pm 0.2\,\mathrm{km\,s}^{-1}$ based on a Gaussian analysis of the H I absorption profile towards Sgr A, and which refers to the slow clouds only. In spite of the errors in these various determinations, the trend is seen to be consistent with the two-population hypothesis. It must be mentioned that in the present analysis we have not explicitly considered the random motions of the H II regions themselves. However, these motions, if they are significant and uncorrelated with those of H I clouds, will reflect in our value of σ_s. In such a case the dispersion estimated by us for the slow clouds will have to be reduced further; in any case, it may be considered an upper limit to the dispersions of both the slow clouds and H II regions. Further as discussed in Paper I, the marked asymmetry of the ΔV distribution shows that the H II region dispersion cannot be larger than that of the slow clouds; this is because the contribution of the H II region dispersion to the distribution has to be symmetric about $\Delta V = 0$.

Fast clouds

As noted in Paper I, independent evidence indicating the presence of two populations of H I clouds has in fact been obtained from an investigation of the H I absorption spectrum towards the galactic centre, a direction free in principle of galactic rotation effects (RS and R&S). R&S have also discussed even earlier evidence in the work of Routly and Spitzer (1952) and Siluk and Silk (1974) suggesting the existence of more than one population of interstellar clouds. From an analysis of the H I absorption spectrum measured towards the galactic centre using the Parkes interferometer RS claimed the existence of a low optical depth, high dispersion ($\sigma \sim 35\,\mathrm{km\,s}^{-1}$) component in this direction. On the basis of this result R&S proposed a two population picture of H I clouds. An attempt made by Schwarz et al. (1982) to verify the results of RS using the Westerbork Synthesis Radio Telescope led to their conluding that any high dispersion ($\sigma \sim 35\,\mathrm{km\,s}^{-1}$) low optical depth feature towards the galactic centre is less than one-third that claimed by RS. In spite of this gross discrepancy it seems to us, in view of the analysis in Sect. III (of the data presented in Paper I), that there do exist H I clouds with velocity dispersion much larger than 4–$5\,\mathrm{km\,s}^{-1}$ estimated for the standard clouds. Further, there are also other observations indicating large peculiar motions of H I clouds, e.g., Silvergate and Terzian (1978) and Shaver et al. (1981). It would appear that the real question is regarding the estimate of the number density and velocity dispersion of such clouds and not of their existence. The accuracy of our estimates are of course subject to selection effects and the small sample used.

We tentatively identify the fast clouds with the high random velocity "shocked clouds" discussed by R&S. But our number densities and dispersions for them, listed in Table 2 are substantially lower than the values suggested by R&S; $n_f \sim 15$–$20\,\mathrm{kpc}^{-1}$ and $\sigma_f \sim 35\,\mathrm{km\,s}^{-1}$. The discrepancies are in fact so large that either one or both estimates of each quantity are severely in error, or they do not refer to the same set of clouds. We discuss below a possible selection effect which could simultaneously explain the discrepancy in both the number density and the dispersion of these fast clouds.

There are a number of good reasons to believe that whatever mechanism accelerates the fast clouds – e.g. supernova shocks – will also heat and partially evaporate them (McKee and Ostriker 1977). Both the reduction in mass and increase in temperature will thus contribute to reducing the H I optical depth of the fast clouds. As discussed by R&S, there is also observational evidence supporting the correlation of high peculiar velocities with higher temperatures and lower optical depths in the measurements of Dickey et al. (1978). As a direct result, any absorption survey will select only a fraction of the fast clouds whose optical depths (and corresponding mean speeds) are within the sensitivity limits of the survey.

The lowest optical depth of the features listed in Table 1 is 0.2, and the distribution of their optical depths indicates a sharp sensitivity cut-off around $\tau \approx 0.3$. The median optical depth for the fast clouds is expected to be of the order of 0.1 or less (R&S). If the number of fast clouds as a function of their optical depth follows an exponential law as is true for the slow clouds (Clark, 1965; Radhakrishnan and Goss, 1972), or falls more steeply as suggested by Crovisier (1981), then we should expect only a very small fraction ($\lesssim e^{-3} \approx 1/20$) of the fast clouds to appear in the data of Table 1. This is in reasonable agreement with the ratio of 0.6 kpc^{-1} found here, to 15–20 kpc^{-1} suggested by R&S.

The cut-off in peculiar velocity as a result of the same selection effect is not as easy to estimate because of the lack of a detailed theory relating cloud acceleration by shocks to their resultant H I optical depths. Even so, given that there exists a correlation of peculiar velocities with optical depth, it seems to us that the reduction in the observed dispersion ($15/35 \approx 40\%$) is not at all surprising for a sample of the optically thickest 5% of the total population of fast clouds. It should be noted that given a sensitivity cut-off, it would in general make it harder to distinguish between two gaussians and a single exponential for the total velocity distribution of the clouds. This has presumably contributed to the choice of an exponential distribution in some earlier analyses. In the present case, however, goodness of fit tests, particularly on the tail of the histogram reject a single exponential distribution with more than 95% confidence.

V. Conclusions

We have made an analysis of the differences between the terminal velocities of H I absorption spectra in the direction of 38 H II regions of known distance, and their recombination line velocities. The analysis has demonstrated that it can provide estimates of the number densities and random velocity dispersions of interstellar H I clouds. The novel method used here has the advantage of operating in a region of velocity space free of the blending effects which plague other types of analysis of similar observations in the galactic plane. The significance of the results obtained is however somewhat limited by the size of the sample. Even so the results support a two-population picture for galactic H I clouds. The values obtained here describing the population of slower and optically thicker clouds are believed to be better than other previous estimates. On the other hand, the number density and dispersion for the population of fast clouds are clearly underestimates because of a selection effect due to a sensitivity cut-off.

While it can be shown that the present and previous estimates for the numbers describing the fast clouds can be reconciled in terms of the selection effect, the overall uncertainties would not warrant an attempt to correct for it. If more sensitive H I absorption measurements could be obtained near the terminal velocities of the spectra of even the present limited sample of sources, the parameters of the fast clouds could be well established. It would therefore be of value to carry out such measurements which we predict will reveal a number of low optical depth ($\tau < 0.1$) features located beyond the terminal velocities in the present data.

Acknowledgements. We thank Rajaram Nityananda and Ramesh Narayan for numerous discussions and helpful suggestions on the method of analysis. We also thank J. Crovisier for useful comments.

Appendix

1. The distribution of cloud velocities

Consider a line of sight to an H II region along which the rate of change of radial velocity with distance (dv/dr) is a constant (the radial velocity increases or decreases linearly with distance). Then given a random distribution of N clouds along this line of sight, each of the clouds will have an equal probability of having any systematic velocity between 0 and the velocity of the H II region ($V_{H II}$). We ignore here large scale density fluctuations such as spiral arms, interarm regions, etc. Then, for each of the clouds the probability distribution of systematic velocity is a rectangular (window) function extending from 0 to the velocity of the H II region.

The 38 H II regions in Paper I were selected all to lie either much nearer than the tangential point or beyond the solar circle (otherwise ΔV values of both signs can occur even in the absence of random motions). Dickey and Benson (1982) have recently observed one of these 38 H II regions (G25.4-0.2) and suggest that it is at the far kinematic distance. If this is true then this source will not meet the above criteria. However, the inclusion of this source in our sample will not seriously alter the derived statistics owing to its small ΔV value.

If an H II region is outside the solar circle, the systematic velocity range for the H I clouds is from the tangential point velocity (V_{TP}) to the velocity of the H II region; but each of the clouds will have twice the probability of having any systematic velocity between 0 and the tangential point velocity. Therefore the probability distribution is a step function, the step being at the solar circle, viz. at a systematic velocity of 0.

Given a systematic velocity, the true velocity of the cloud will be given by a Gaussian probability distribution function of dispersion σ centred on this systematic velocity. Clearly, the overall probability distribution for the velocity of any cloud is the convolution of the systematic velocity distribution and the random velocity distribution.

Mathematically, for any cloud the total probability distribution for the velocity difference between the H II region and it is given by

$$p_T(\Delta V) = p_{sys} * p_{ran} = \int_{-\infty}^{\infty} p_{sys}(\Delta V') p_{ran}(\Delta V - \Delta V') d\Delta V' . \qquad \text{(A1)}$$

p_{ran} is the random velocity distribution given by

$$p_{ran}(\Delta V - \Delta V') = \frac{1}{\sigma\sqrt{2\pi}} \exp -(\Delta V - \Delta V')/2\sigma^2 .$$

p_{sys} is the systematic velocity distribution (the window function) obtained as described below.

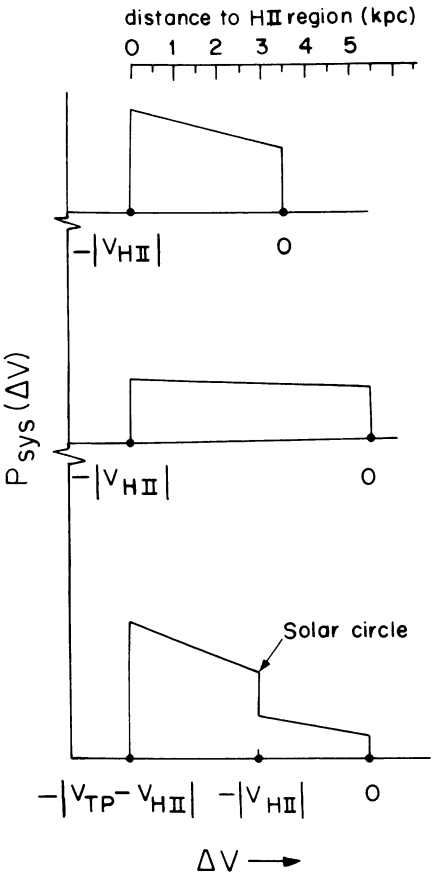

Fig. 6. Typical probability distribution (the window function) of systematic velocity with respect to the H II region of any cloud lying along the line of sight to it. The one with a step is for an H II region outside the solar circle

In general, dv/dr varies as a function of distance (therefore as a function of velocity) and equal intervals in velocity space will not have equal probabilities. The probability of a cloud having a certain systematic velocity, and thus the number of clouds, will be inversely proportional to $|dv/dr|$ at that velocity.

According to the Schmidt model of galactic rotation, $1/|dv/dr|$ varies smoothly as a function of distance (therefore as a function of velocity) except near the tangential point. If we ignore a small stretch near the tangential point, then the probability distribution function can be approximated by a trapezoidal window function. Some typical window functions are illustrated in Fig. 6. The one with a step is for an H II region outside the solar circle.

The probability distribution of ΔV for each of the clouds is then given by the convolution of a trapezoidal window function such as shown in Fig. 6, with the Gaussian probability distribution of peculiar velocities. If p_{Ts} is the total probability function for slow clouds computed in this fashion, and p_{Tf} is the total probability function of the fast clouds, then the Eq. (2) for the overall probability distribution of ΔV can be written as

$$P(\Delta V)=N_s p_{Ts} P_{Ts}^{N_s-1} P_{Tf}^{N_f} + N_f p_{Tf} P_{Tf}^{N_f-1} P_{Ts}^{N_s}, \qquad \text{(A2)}$$

where

$$P_{Ts}=\int_{-\infty}^{\infty} p_{Ts}\, d\Delta V'$$

$$P_{Tf}=\int_{-\infty}^{\infty} p_{Tf}\, d\Delta V'.$$

Equation (A2) can now be used for computing the probability distribution of ΔV for individual H II regions. As noted earlier, if random motions of H I clouds are the origin of their apparently anomalous distances, we would expect a finnite probability of finding large positive ΔV values for those H II regions which are distant and have a small $|dv/dr|$ along the line of sight. In other words, large positive values of ΔV can occur for those sources for which the window functions are of large widths or heights or both.

It should however be pointed out here that the exact probability distribution will depend on the number density and σ of the two populations. In the extreme case of very large number density and σ, there is always a high probability of large ΔV values irrespective of dv/dr and distance. But given reasonable number densities, and σ of the order indicated in Paper I, we show in the text that the probability functions for ΔV in individual cases do indeed depend on the window functions.

2. Goodness of fit and estimation of errors

To obtain the best fit values of the parameters n_s, σ_s, n_f, and σ_f (or n and η for the exponential distribution) which correspond to the maximum value of the joint probability P [Eq. (3)] we have minimized the quantity

$$-\log P=\sum_{i=1}^{38} -\log P_i(\Delta V_i). \qquad \text{(A3)}$$

The expectation value of $-\log P_i$ for the i^{th} H II region is given by

$$\langle -\log P_i\rangle=\int_{-\infty}^{\infty} (-\log P_i) P_i\, d\Delta V$$

and its variance is given by

$$\sigma_P^2=\int_{-\infty}^{\infty} (-\log P_i-\langle -\log P_i\rangle)^2 P_i\, d\Delta V.$$

We define

$$\Psi^2=\frac{N}{N-K}\sum_{i=1}^{38} (-\log P_i-\langle -\log P_i\rangle)^2/\sigma_P^2, \qquad \text{(A4)}$$

where $N-K$ is the number of degrees of freedom left after fitting K parameters to N data points ($N=38$).

The quantity Ψ^2 can be considered as a measure of goodness of fit and similar to the conventional χ^2. For a good fit the value of Ψ^2 must be close to N. The value of Ψ^2 computed using the best fit values for the two-gaussian and a single exponential distribution of velocities of H I clouds is given in Table 2.

The parameters n_s, σ_s, n_f and σ_f (n and η for the exponential distribution) of the fit using the maximum likelihood method [of maximizing the joint probability P, Eq. (3)] are not independent. The variation of $-\log P$ [Eq. (A3)] as a function of one of the parameters depends on how well the other parameters have been fitted. We have estimated the errors in each of the parameters assuming that the variation of $-\log P$ is parabolic, at least near its minimum, and taking into account the correlation between these variations with respect to different parameters. The errors quoted in Table 2 correspond to one standard deviation.

References

Adams, W.S.: 1949, *Astrophys. J.* **109**, 354
Blaauw, A.: 1952, *Bull astr. Inst. Netherl.* **11**, 459
Clark, B.G.: 1965, *Astrophys. J.* **142**, 1398
Crovisier, J.: 1978, *Astron. Astrophys.* **70**, 43
Crovisier, J.: 1981, *Astron. Astrophys.* **94**, 162
Dickey, J.M., Salpeter, E.E., Terzian, Y.: 1978, *Astrophys. J. Suppl.* **36**, 77
Dickey, J.M., Benson, J.M.: 1982, *Astron. J.* **87**, 278
McKee, C.F., Ostriker, J.P.: 1977, *Astrophys. J.* **218**, 148
Radhakrishnan, V., Goss, W.M.: 1972, *Astrophys. J. Suppl.* **24**, 161
Radhakrishnan, V., Sarma, N.V.G.: 1980, *Astron. Astrophys.* **85**, 249
Radhakrishnan, V., Srinivasan, G.: 1980, *J. Astrophys. Astron.* **1**, 47
Routly, P.M., Spitzer, L. Jr.: 1952, *Astrophys. J.* **115**, 227
Schwarz, U.J., Ekers, R.D., Goss, W.M.: 1982, *Astron. Astrophys.* **110**, 100
Shaver, P.A., Retallack, R.S., Wamsteker, W., Danks, A.C.: 1981, *Astron. Astrophys.* **102**, 225
Shaver, P.A., Radhakrishnan, V., Anantharamaiah, K.R., Retallack, D.S., Wamsteker, W., Danks, A.C.: 1982, *Astron. Astrophys.* **106**, 105
Silvergate, P., Terzian, Y.: 1978, *Astron. J.* **83**, 1412
Siluk, R.S., Silk, J.: 1974, *Astrophys. J.* **192**, 51